STACKING RADAR SEARCH FENCES FOR INCREASED RANGE IN SPACE SITUATIONAL AWARENESS

Hans Schily and Isabel Schlangen

Fraunhofer FKIE, 53343 Wachtberg, Germany, Email: {hans.schily, isabel.schlangen}@fkie.fraunhofer.de

ABSTRACT

Targets orbiting Earth typically are either far away and slowly pass a search fence or closer to the radar and pass very quickly. This behaviour of targets can be exploited when designing a radar search fence to better distribute the radiated power within the search volume. This paper presents a method for designing a radar search fence that is stacked at different ranges within the same angular search space of the radar. A simple simulative study using publicly available data on low Earth orbit targets is conducted to compare the search fence with its non-stacked version. The simulation shows that it can be a better alternative compared to reducing dwell durations to free up radar resources, if the number of objects detected is a priority.

Keywords: radar; search fence; space situational awareness.

1. INTRODUCTION

Radar is a valuable resource for near-Earth space situational awareness. Due to its all-weather capability and ability to cover a large field of regard, it is particularly useful for finding new targets that are not yet known from previous observations or an external catalogue. A common mode of operation is to have the radar repeat a fixed beam pattern, forming a search fence that captures unknown targets in a systematic way. This search fence is designed to detect all targets within its predetermined search volume with a given probability.

The exact configuration of the search fence depends on the radar's capabilities and a target model. Each beam in the set of beams that constitute the search fence has its individual dwell time such that a target will be detected up to a predetermined range. In addition, the beam pattern of the fence must repeat within a set time, so that all targets crossing the fence are captured. The limited time and power budget of the radar then creates a trade-off between the maximum range and angular space that the search fence can cover to find targets specified by the target model.

The idea of spanning a radar search fence to detect objects orbiting earth was implemented shortly after the launch of the first spacecraft [12]. Since then space fences became a proven technology for space situational awareness with the task to build and maintain a catalogue of objects orbiting Earth [2, 3, 12]. Recent literature analyses a double fence system, where the beams form a V-shape and proposes a method to correlate detections in both parts of the fence by considering orbital constraints [4].

Operating a radar with a simple search fence may not make the best use of the sensor's available resources. This paper considers a technique in which the radar search beam pattern is augmented to include two search fences that are stacked at different ranges within the same angular search space of the radar. Assuming stable orbits, targets at low altitudes are expected to spend less time within the search fence because they move faster and travel a shorter distance to cross the search fence. In contrast, targets at higher altitudes are expected to move more slowly while travelling a larger distance within the search fence. Thus, low-altitude targets require a shorter dwell time, and the radar must revisit the beams of the search fence more quickly. For high-altitude targets, the radar requires a longer dwell duration but also has more time available to cover the entire search fence. Hence, there is potential in dividing the search space into two separate range domains. One fence covers the search space from a minimum to a cut-off distance, while the second fence finds targets at ranges greater than the cut-off distance. This work describes a method for finding optimised parameters for a stacked search fence and conducts a simple simulative study using publicly available data on low Earth orbit (LEO) targets to compare the stacked search fence with its non-stacked version.

2. SYSTEM MODEL

The search performance of the radar is modelled with the surveillance radar equation [8]

$$\text{SNR} = \frac{P_{av} A \sigma}{16 R^4 k_b T L} \frac{t_{sc}}{\Omega} \,. \tag{1}$$

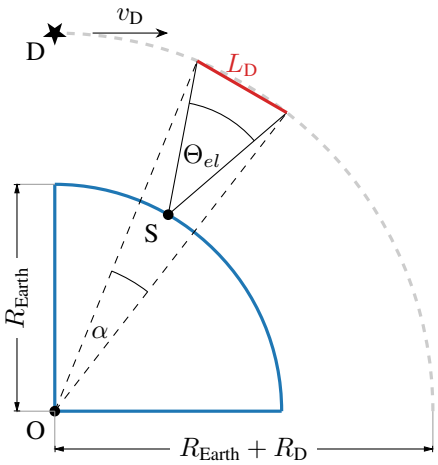

Figure 1. Search fence geometry. A radar station (S) observes a target (D) orbiting Earth (blue). The search fence has an elevation angle of Θ_{el} and is directed towards the zenith, while the target follows a circular orbit (grey) with speed v_D. The shortest path L_D for a target passing the fence is marked in red.

Here we assume an average power P_{av}, antenna aperture A, target radar cross section (RCS) σ, scanning time t_{sc}, target range R, Boltzmann constant k_b, system temperature T, system losses L and solid angle Ω, which constitutes a search area in the angular domain, to result in the signal-to-noise ratio (SNR) for target detection. The radar requires scanning time t_{sc} to search the volume defined by R and Ω. Factoring the solid angle

$$\Omega = \Theta_{el}\Theta_{az} \tag{2}$$

into a product allows us to describe the search fence in terms of two angles, Θ_{az} and Θ_{el} in azimuth and elevation direction, respectively.

Figure 1 sketches a cut through the search fence in the plane of Θ_{el}. We assume the target to move along the cut plane. Naturally, most targets will follow other trajectories depending on the orbital parameters of the target and the orientation of the search fence. The target D is on a stable orbit with speed v_D. Radar station S intercepts the target with its search fence at an altitude of R_D. The search fence points towards the zenith.

Rearranging (1) provides the scanning time the radar requires to detect a target with RCS σ and at a range smaller R_max within the search fence

$$t_{sc} = \mathrm{SNR}\ \Omega\ \frac{16 R_\mathrm{max}^4 k_b T L}{P_{av} A \sigma}\ . \tag{3}$$

If the radar should not miss a target passing the fence, the time available to search the fence t_{av} is limited. It depends on the path taken by the target and the target's speed. Using pessimistic, but reasonable assumptions, we let the target pass through the fence along Θ_{el}

$$L_\mathrm{D} = 2R_\mathrm{D} \sin\left(\frac{\Theta_{el}}{2}\right)\ . \tag{4}$$

The speed of the target is [7]

$$v = \sqrt{GM\left(\frac{2}{R_\mathrm{Earth} + R_\mathrm{D}} - \frac{1}{a}\right)}\ , \tag{5}$$

assuming a semi-major axis of length a and with the gravitational constant G and mass M. Furthermore, assuming a maximum eccentricity e of 0.25 and observing the target, in the worst case, at its periapsis, the resulting target speed is

$$v_\mathrm{D} = \sqrt{GM\frac{1.25}{R_\mathrm{Earth} + R_\mathrm{D}}}\ . \tag{6}$$

Hence, the radar has time

$$t_{av} = \frac{2R_\mathrm{D}\sin\left(\frac{\Theta_{el}}{2}\right)}{\sqrt{GM\frac{1.25}{R_\mathrm{Earth}+R_\mathrm{D}}}} \tag{7}$$

available to search for target D. The available search time decreases for low-altitude targets.

From (3) and (7) we find that the distance to the target determines the scanning time t_{sc} and the available time t_{av}. The time budget $0 \leq \rho \leq 1$ the radar can spend searching for targets

$$\rho = \frac{t_{sc}}{t_{av}} \tag{8}$$

$$= \mathrm{SNR}\ \Omega\ \frac{16 R_\mathrm{max}^4 k_b T L}{P_{av} A \sigma}\ \frac{\sqrt{GM\frac{1.25}{R_\mathrm{Earth}+R_\mathrm{min}}}}{2R_\mathrm{min}\sin\left(\frac{\Theta_{el}}{2}\right)}\ , \tag{9}$$

must respect the minimum R_min and maximum range R_max of the search fence.

This raises the question of whether there exist partitions in range that minimise the time spent searching while leaving all other system and target parameters fixed.

3. SEARCH FENCE PARTITIONING

In the simplest case, the search fence is split into two distinct layers at $R_\mathrm{min} < R_\mathrm{split} < R_\mathrm{max}$. The resource reduction factor Γ measures the reduction in time budget required for searching

$$\Gamma = \frac{\rho_\mathrm{L} + \rho_\mathrm{U}}{\rho_\mathrm{S}} \tag{10}$$

by normalizing the resources required for serving an upper and lower search fence $\rho_\mathrm{L} + \rho_\mathrm{U}$ with the time budget required for a fence with a single layer ρ_S. Equation (9) provides the time budget for ρ_S while the lower fence requires a budget of

$$\rho_\mathrm{L} = \mathrm{SNR}\ \Omega\ \frac{16 R_\mathrm{split}^4 k_b T L}{P_{av} A \sigma}\ \frac{\sqrt{GM\frac{1.25}{R_\mathrm{Earth}+R_\mathrm{min}}}}{2R_\mathrm{min}\sin\left(\frac{\Theta_{el}}{2}\right)} \tag{11}$$

and the upper fence

$$\rho_{\mathrm{U}} = \mathrm{SNR}\,\Omega\,\frac{16R_{\max}^4 k_b T L}{P_{av} A \sigma}\frac{\sqrt{GM\frac{1.25}{R_{\mathrm{Earth}}+R_{\mathrm{split}}}}}{2R_{\mathrm{split}}\sin\left(\frac{\Theta_{el}}{2}\right)}\,. \quad (12)$$

It follows that

$$\Gamma = \left(\frac{R_{\mathrm{split}}}{R_{\max}}\right)^4 + \frac{R_{\min}\sqrt{R_{\mathrm{Earth}}+R_{\min}}}{R_{\mathrm{split}}\sqrt{R_{\mathrm{Earth}}+R_{\mathrm{split}}}}\,. \quad (13)$$

Note that the reduction in resources for searching the fence only depends on the involved minimum, maximum, and split ranges as well as Earth's radius. Also, observe that the second derivative of (13) is positive for positive R_{split}, so we expect a convex function that must provide a minimum value $\Gamma^\star$ for R_{split} in the interval $(R_{\min}, R_{\max})$, although it is not guaranteed that $\Gamma^\star < 1$, that is, splitting the fence saves radar resources.

In addition, (13) can be generalized to splitting the fence into N parts

$$\Gamma(N) = \sum_{n=0}^{N-1}\left(\frac{R_{n+1}}{R_N}\right)^4 \frac{R_0}{R_n}\frac{\sqrt{R_{\mathrm{Earth}}+R_0}}{\sqrt{R_{\mathrm{Earth}}+R_n}}\,, \quad (14)$$

where $R_0 < R_1 < \ldots < R_N$. However, it is unclear whether splitting the fence into more than two layers makes sense. This work focuses on a two-layered search fence. Investigating further splitting of the search volume is left for future work. However, (14) is shown for completeness.

As an example, for $R_{\min} = 300\,\mathrm{km}$ and $R_{\max} = 1500\,\mathrm{km}$ the time budget required for searching the fence can be reduced significantly to less than half of the original time budget (cp. Figure 2). However, also note that splitting the search fence close to the maximum range requires more resources than using the original single-layer search fence.

Figure 3 illustrates the dependency of $\Gamma^\star$ on the depths of the search volume $\frac{R_{\min}}{R_{\max}}$ and the maximum search distance $R_{\max}$. As expected, search fences with $R_{\min} << R_{\max}$ benefit the most from being split. If $R_{\min} \gtrsim 0.5 R_{\max}$, there is no longer a significant reduction in resources from splitting the fence. The dependency of $\Gamma^\star$ on $R_{\max}$ is negligible compared to the dependency on search depths for the parameters as plotted in Figure 3.

Inspecting (1), it is clear that the new time budget, available by introducing a layered search fence, may be used for various purposes. We could increase the azimuth width Θ_{az} of the search volume, increase the maximum search range $R_{\max}$, or invest time in other system functions, such as tracking or confirmation of a target. Using the time budget to increase the sensitivity of the search fence to targets with small RCS is a more complicated problem. The RCS σ from (1) specifies the RCS of a target at $R_{\max}$ that is expected to return a radar echo

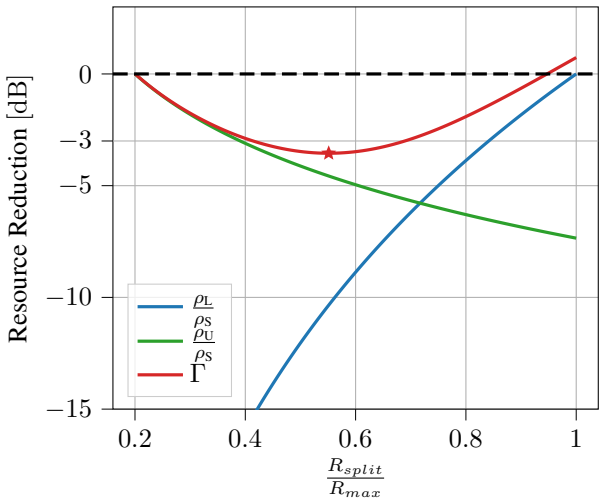

Figure 2. Resource reduction factor Γ for a search fence with $R_{\min} = 300\,\mathrm{km}$ and $R_{\max} = 1500\,\mathrm{km}$. Splitting the search fence more than halves the time required for searching. A Γ below the black dashed line indicates that splitting the search fence into two layers is advantageous.

with the specified SNR and the parameters of the system and the search volume given. Naturally, any target with identical RCS at a distance smaller than $R_{\max}$ returns a stronger echo. Similarly, the sensitivity of the search fence increases with decreasing range. This explains where the resource reduction originates. By splitting the search volume in the range domain, we allow for a decreased sensitivity of the search fence in its lower layers. This trade-off is inherent to this technique. We buy sensor time by decreasing the sensitivity in regions closer to the radar, focusing the search on targets with a minimum RCS of the design parameter σ at both, high and low altitudes.

Illustrating this trade-off requires an estimate of the minimum SNR for target detection. Following [10] and assuming non-fluctuating targets and coherent integration of the radar pulses we employ

$$p_d = Q_M\left(\sqrt{2\mathrm{SNR}}, \sqrt{-2\log p_{fa}}\right)\,, \quad (15)$$

where Q_M is the Marcum's Q function, to find a target SNR value of $14\,\mathrm{dB}$ for a probability of detection p_d of $99\,\%$ and a false alarm rate p_{fa} of 10^{-5}.

To see how the RCS changes with range and a split in the search volume, we can define a nominal RCS value σ_0 that corresponds to the RCS of a target at $R_{\max}$ matching the required SNR_d of $14\,\mathrm{dB}$ for the single layer search fence

$$\sigma_0 = \mathrm{SNR}_d\,\Omega\,\frac{16R_{\max}^4 k_b T L}{P_{av} A}\frac{\sqrt{GM\frac{1.25}{R_{\mathrm{Earth}}+R_{\min}}}}{2R_{\min}\sin\left(\frac{\Theta_{el}}{2}\right)}\,. \quad (16)$$

The range dependent minimum RCS of a detectable tar-

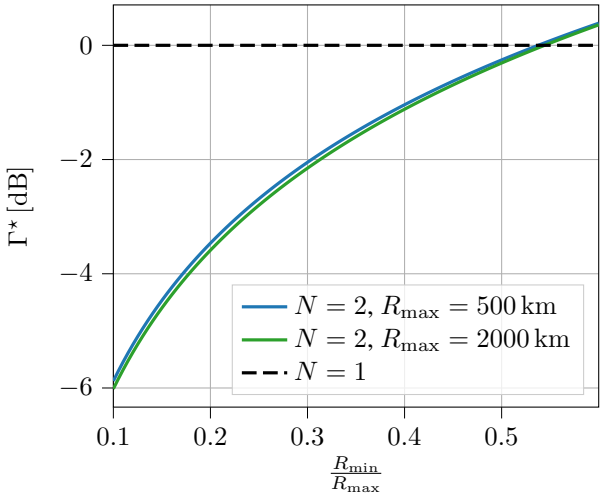

Figure 3. Resource reduction over search fence depth $\frac{R_{\min}}{R_{\max}}$ when choosing the optimal distance to split the fence into two layers. The dependency on the fence's depth is much stronger than the dependency on the maximum search range $R_{\max}$.

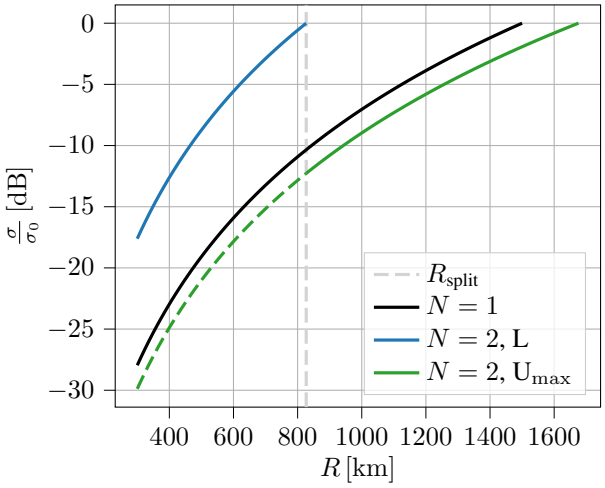

Figure 4. Comparison of minimum detectable RCS of the single layer fence ($N = 1$) and a split fence with two layers ($N = 2$). Investing the time budget available from splitting the search fence into the integration time of the upper fence (U) decreases the minimum detectable RCS.

get for the single layer search fence is a function of σ_0

$$\sigma(R) = \sigma_0 \left(\frac{R}{R_{\max}} \right)^4 . \tag{17}$$

Similarly the RCS for the lower fence is

$$\sigma_L(R) = \sigma_0 \left(\frac{R}{R_{\text{split}}} \right)^4 . \tag{18}$$

The reduction in the required time budget for the split fence is in part due to the availability of more time to search the upper volume. However, the power and integration time that the radar has to invest is the same as for the single-layer search fence. Hence, the RCS profile $\sigma_U(R)$ for the upper layer is identical to the single layer fence RCS profile $\sigma(R)$. If the radar is capable of spending the newly available time on coherently integrating more pulses in the upper layer, the detectable RCS of the search fence reduces to

$$\sigma_{U,\max}(R) = \sigma_0 \left(\frac{R}{R_{\max}} \right)^4 (2 - \Gamma)^{-1} , \tag{19}$$

since the radar can integrate longer by a factor of $2 - \Gamma$, which reduces the nominal RCS by the inverse of that factor. Note that the upper search fence uses the same integration time as the single-layer search fence, since both must reach a range of $R_{\max}$. Therefore, the scaling is applied directly, although Γ is normalised with respect to the single-layer search fence. Correspondingly, the extended maximum range until the minimum detectable RCS limits the search is

$$R_+ = R_{\max} (2 - \Gamma)^{\frac{1}{4}} . \tag{20}$$

Figure 4 compares the minimum detectable RCS for a split search fence using the numbers from the example of Figure 2. The reduction in time required for scanning the split search volume originates in a higher minimum detectable RCS in the lower part of the split search fence. If this time budget is invested to boost the upper fence ($\mathrm{U}_{\max}$), its sensitivity increases together with the maximum range at which a standard target is detected. The maximum range increases about $10\,\%$ in this example.

4. SIMULATION

To gain a better understanding of the effects of splitting a search fence into two layers, we run a simplified simulation. We evaluate three different configurations. The first is the reference search fence with $N = 1$ layers that operates with the full time budget ($\rho = 1$). Second, we implement a search fence that also has a single layer ($N = 1$), but with reduced resources ($\rho = 0.8$). The third search fence is split into two layers ($N = 2$) and also operates on a lower time budget ($\rho = 0.8$). All options use a minimum search range $R_{\min}$ of $200\,\mathrm{km}$ and a maximum search range $R_{\max}$ of $1000\,\mathrm{km}$. The two layered search fence is split at $R_{\text{split}} = 250\,\mathrm{km}$. With that, we aim to confirm the hypothesis that it is better to split the fence into two layers than to reduce the integration time if the available time budget for searching is limited. The rationale is that through reducing the integration time over the full range we might lose more targets than through reducing the integration time only in the lower layer of a multi-layered fence. Note that we can use the upper part of the fence to also cover the lower part with high sensitivity. However, in that case, the guarantee to intercept every object that behaves according to the motion model in the lower fence layer is lost.

The simulation uses publicly available RCS data on objects in LEO from [5]. The data set provides values on

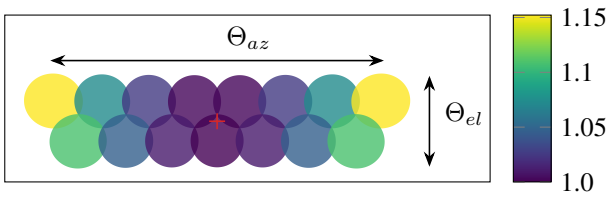

Figure 5. Search fence $3\,\mathrm{dB}$ *beams seen from above the antenna plane. The colour indicates weights* ω_b *scaling the dwell duration to compensate for the reduction in aperture size and element gain, when steering a been of boresight. A red cross indicates the antenna's origin.*

the RCS, apogee altitude, perigee altitude, orbital period, and inclination for many objects that have been or currently are orbiting Earth. Since we are only interested in LEO targets that are within the range of the sensor, a filter reduces the number of targets to those that have:

- an orbital period smaller than $128\,\mathrm{min}$
- a perigee and apogee altitude between $200\,\mathrm{km}$ and $1200\,\mathrm{km}$
- an inclination above $50°$.

This results in a scenario with 17050 objects in LEO. Using [9], we build Kepler orbits from the data by augmenting the missing orbital elements *argument of perigee*, *longitude of the ascending node* and *true anomaly* with uniformly sampled random angles in the interval $[0, 2\pi]$. In this way, using an analytical propagator, the simulation can find all objects present within a radar beam at an arbitrary time during the simulated $2\,\mathrm{h}$ search campaign.

The radar is located at a latitude of $50°\mathrm{N}$ pointing towards the zenith. Since part of target orbit parameters are randomized, the longitude does not matter for this simulation. Figure 5 shows the beams of a phased array antenna that constitute the search fence. In two bars, 15 beams, each with a width $\Theta_{3\,\mathrm{dB}}$ of $5°$, illuminate the sky iterating from East to West and back. Together, they cover an elevation of $\Theta_{el} = 8.7°$ and an azimuth of about $\Theta_{az} = 35.3°$. The beams are arranged on a triangular lattice in antenna coordinates (direction cosine) with a spacing of 0.85 [6]. Since the aperture of an array antenna reduces when seen from an angle, we have to account for additional beam-steering losses. Therefore, we introduce a factor

$$\omega_b = \cos^4(\beta) \tag{21}$$

that models the additional integration time required to compensate for the array losses as well as additional losses from an individual antenna element, where β is the steering angle of the radar beam. Figure 5 illustrates these factors in terms of colour.

First, the simulation sets a schedule for the radar beams based on the fence design parameters using the *earliest deadline first* [1] scheduler. The time available to iterate all beams of a layer is known from (7). We define the nominal dwell durations of the beams as

$$\tau_{b,0} = \frac{t_{av}(R_{\min})\omega_b}{15\ \sum_{b=1}^{15} \omega_b}\ . \tag{22}$$

We assume the radar to detect a target with RCS $\sigma_0 = 0\,\mathrm{dB\,m^2}$ at a range of $R_{\max} = 1000\,\mathrm{km}$ with dwell durations $\tau_{b,0}$. Hence, (17) provides the detectable RCS at range R. If we split the search fence into two layers, the dwell durations for the beams of the lower fence require adaption. Since they only need to detect objects with $\sigma_0 = 0\,\mathrm{dB\,m^2}$ at $R_{\text{split}} = 250\,\mathrm{km}$, the beam dwell durations reduce to

$$\tau_{b,\mathrm{L}} = \tau_{b,0} \left(\frac{R_{\text{split}}}{R_{\max}} \right)^4 . \tag{23}$$

Consequently, for the lower fence, objects require a minimum RCS described by (18). Note that the dwell durations for the beams in the upper and lower fences may differ by a large factor. A radar implementing this technique must be able to produce very short as well as long dwells in rapid succession.

The deadlines required by the scheduler then compute to

$$\tau_{\text{EDF}} = t_0 + t_{av} - \sum_{b=i}^{15} \tau_b\ , \tag{24}$$

where i is the index of the i-th beam and t_0 the start time of the current search beam sequence. Therefore, by tracking the index of the current beam, each search fence task can provide execution deadlines to the scheduler.

From the schedule, the simulation samples the Kepler orbits of the targets to test for interception. As described above, targets with a larger RCS than found by (17, 18) are declared detections. Figure 6 highlights the resulting set of detected LEO objects for the single layer search fence with full resources in red. We can see that there is a significant number of targets in the small RCS range that is not covered by the single layer fence at reduced resources (green). Furthermore, there exist many known objects with small RCS at low ranges. The lower fence of the two-layer fence cannot find these targets. However, if these objects cross the search fence on a trajectory that gives the search fence more time for detection than assumed in the model (7), the upper layer of the fence may catch them. Note that the lower layer only gives the guarantee of finding fast targets with a high RCS, while the upper layer can still be used to find slow targets at low altitude with a low RCS.

Table 1 confirms this observation. Both fences using reduced resources generate fewer detections and find fewer objects. Splitting the search fence reduces detections, but increases the number of objects intercepted with the fence. Since the single-layered search fence with reduced resources more frequently samples the low-altitude regions, where many known targets reside, it generates more detections. However, it misses targets with small

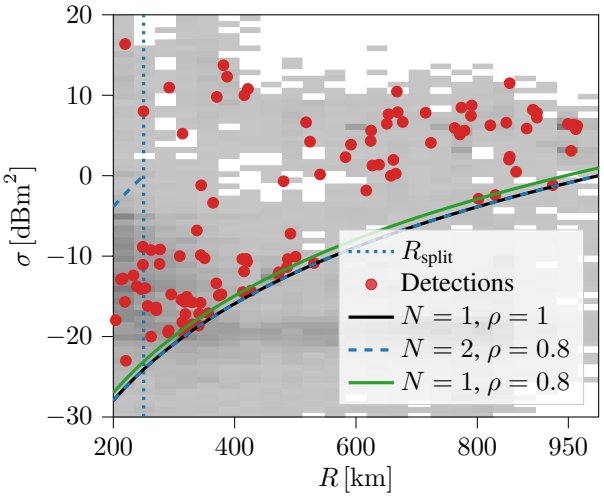

Figure 6. Simulation results for three different search fence setups. A search fence with a single layer ($N = 1$, $\rho = 1$, black), a single layered search fence with a reduced time budget ($N = 1$, $\rho = 0.8$, green) and a double layered search fence with a reduced time budget ($N = 2$, $\rho = 0.8$, dashed blue). The double layered search fence uses the single layered search fence with full resources as its upper part. In red are the objects detected by the single layered search fence at full resources. The background provides a histogram of objects used for the simulation.

RCS over the full range when compared to the search fence using the full time budget. The two-layer split search fence still captures slow targets at low altitudes, while also finding low RCS objects, therefore detecting more targets in total. Of course, these results strongly depend on the distribution of the known and publicly available objects in LEO. Different data on the target distribution may lead to other results.

Based on the simulation, we conclude that a modern radar that has to trade time from its search function to serve other tasks like tracking or object confirmation can use this method of a split search fence to make the best use of the remaining time budget. While the guarantee to find all fast-moving targets at low altitude and RCS is lost, the simulation shows that it is a better alternative compared to reducing dwell durations, if the number of objects detected is a priority.

Table 1. Comparison of results for a single layer fence with full resources ($N = 1$, $\rho = 1$), a single layer fence with reduced resources ($N = 1$, $\rho = 0,8$) and a two layered fence with reduced resources ($N = 2$, $\rho = 0.8$). Detections sum all objects detected throughout the simulation run, while the object IDs column counts the unique identifiers of detected targets crossing the search fence.

Fence type	Detections	Object IDs
$N = 1, \rho = 1$	399	121
$N = 1, \rho = 0.8$	**365**	108
$N = 2, \rho = 0.8$	317	**115**

5. CONCLUSION

The study highlights the advantages and disadvantages of the stacked search fence and shows that it does indeed find more targets. However, the search fence also loses sensitivity when searching at low altitudes. In conclusion, there is a trade-off when designing a search fence where the effective range of the search can be increased for targets with an RCS that is larger than assumed in the target model, but consequently the probability of detecting small RCS targets is reduced at lower ranges. If the radar time budget is limited, splitting the search fence is the better approach to saving time compared to reducing the dwell duration of the search beams, because it finds more objects.

ACKNOWLEDGMENTS

The project on which this report is based was funded by the German Federal Ministry for Economic Affairs and Climate Action under the funding code 50 LZ 2005. Responsibility for the content of this publication lies with the author.

REFERENCES

1. Buttazzo G., (1997). *Hard real-time computing systems*, Springer
2. Fonder G., et al., (2019). Space fence radar overview. *2019 International Applied Computational Electromagnetics Society Symposium (ACES)*, 1–2), IEEE.
3. Haimerl J. A., Fonder G. P., (2015). Space fence system overview. *Proceedings of the Advanced Maui Optical and Space Surveillance Technology Conference*, 1–3, Curran Associates Inc.
4. Huang J., et al., (2012). A novel data association scheme for LEO space debris surveillance based on a double fence radar system. *J. Adv. Space Res.*, Elsevier
5. Kelso T. S., (2024). *SATCAT Format Documentation*. https://celestrak.org/satcat/satcat-format.php
6. Klemm, Richard, et al., (2017). *Novel radar techniques and applications volume 1: real aperture array radar, imaging radar, and passive and multistatic radar*, SciTech
7. Logsdon T., (1997). *Orbital mechanics: theory and applications*, John Wiley & Sons
8. Mahafza Bassem R., (2005). *Radar systems analysis and design using MATLAB*, Chapman and Hall/CRC

9. Maisonobe L, et al., (2010). Orekit: An open source library for operational flight dynamics applications, *4th international conference on astrodynamics tools and techniques*, 3–6

10. Richards M., Scheer J., et al., (2010). *Principles of modern radar*, SciTech

11. Settecerri T. J., et al., (2004). Analysis of the Eglin radar debris fence. *Acta Astronautica*, 54(3), 203–213.

12. Sridharan R., Pensa A. F., (1998). Us space surveillance network capabilities. *Image Intensifiers and Applications; and Characteristics and Consequences of Space Debris and Near-Earth Objects*, 88–100, SPIE